Direct bandgap germanium-on-silicon inferred from 5.7% ⟨100⟩ uniaxial tensile strain [Invited]

David S. Sukhdeo,[1] Donguk Nam,[1,*] Ju-Hyung Kang,[2] Mark L. Brongersma,[2] and Krishna C. Saraswat[1]

[1]*Department of Electrical Engineering, Stanford University, Stanford, California 94305, USA*
[2]*Department of Materials Science and Engineering, Stanford University, Stanford, California 94305, USA*
**Corresponding author: dwnam@stanford.edu*

Received February 3, 2014; accepted March 5, 2014;
posted March 6, 2014 (Doc. ID 205862); published April 11, 2014

We report uniaxial tensile strains up to 5.7% along ⟨100⟩ in suspended germanium (Ge) wires on a silicon substrate, measured using Raman spectroscopy. This strain is sufficient to make Ge a direct bandgap semiconductor. Theoretical calculations show that a significant fraction of electrons remain in the indirect conduction valley despite the direct bandgap due to the much larger density of states; however, recombination can nevertheless be dominated by radiative direct bandgap transitions if defects are minimized. We then calculate the theoretical efficiency of direct bandgap Ge LEDs and lasers. These strained Ge wires represent a direct bandgap Group IV semiconductor integrated directly on a silicon platform. © 2014 Chinese Laser Press

OCIS codes: (160.3130) Integrated optics materials; (160.3380) Laser materials.
http://dx.doi.org/10.1364/PRJ.2.0000A8

1. INTRODUCTION

With traditional copper interconnects becoming an ever greater performance bottleneck [1], optical interconnects have become an increasingly attractive option for silicon (Si) integrated circuits [2]. Although Si's indirect bandgap limits its ability to perform optoelectronic functions for photonic integrated circuits, there is a strong interest in using germanium (Ge) for such functions since Ge can be monolithically integrated on Si and shows superior optical properties compared to Si [3–6]. Although Ge is also an indirect bandgap semiconductor, it also has a direct bandgap that is only ~140 meV larger than its indirect gap [7], and this property has enabled the realization of efficient Ge photodetectors [8–10] and modulators [11].

However, Ge's indirect bandstructure has proven acutely problematic for lasing, forcing researchers to explore options such as heavy n-type doping [12–14] and tensile strain [9,12,15,16]. The first of these methods, n-type doping, mitigates the presence of indirect conduction band states by filling them with extrinsic electrons [12,17]. Tensile strain, on the other hand, works by favorably altering Ge's bandstructure until it becomes a direct bandgap semiconductor at ~4.6% uniaxial strain along ⟨100⟩ [7] as shown in Fig. 1. While an electrically pumped Ge laser has been demonstrated using heavy n-type doping and a very small tensile strain [18], this laser suffered a very high threshold current density such that substantial improvements are necessary before practical applications are possible. For applications where operation outside the telecom wavelength of 1550 nm is acceptable, it has been theoretically shown that employing a much larger tensile strain and making Ge's bandstructure approach a direct bandgap is the most promising route to achieving an efficient low-threshold Ge laser [17].

In this work we present Ge wires, supported on Si substrates, with uniaxial tensile strains as high as 5.7% along the ⟨100⟩ axis. These wires were fabricated in a manner similar to the technique of [19], but using high-quality germanium-on-insulator (GOI) substrates to increase the maximum achievable strain before material fracture.

2. MATERIALS AND METHODS

To begin, a GOI substrate is fabricated using the method of [20]. The Ge was originally grown heteroepitaxially on Si, which results in baseline tensile strain of ~0.2% after cooling down from growth temperatures due to a mismatch of the thermal expansion coefficients [21]. This tensile strain remains after bonding onto a Si/SiO_2 wafer to create the GOI substrate [20,22]. The use of GOI provides substantial benefits over using Ge-on-Si as in [19] because the use of GOI eliminates the Ge/Si interface [20], which is known to be highly defective due to the lattice mismatch between Ge and Si [23]. Not only is the material quality important from a carrier lifetime and device performance perspective, but material defects such as threading dislocations are known to reduce material strength and hence reduce the maximum achievable strain before material fracture [24]. We therefore hypothesize that the use of GOI is the key reason why we observe substantially more strain than other researchers who employed a similar technique [19].

Using this GOI, a pad and nanowire geometry similar to [19,22] was patterned using e-beam lithography and dry etching in SF_6 and $CHClF_2$ (Freon-22) plasma. The underlying oxide was then etched in HF vapor, releasing the structure to give a suspended Ge wire attached on either side to suspended Ge pads as shown in Fig. 2(a). Typical wire dimensions were ~4.5 μm × ~200 nm, as shown in Fig. 2(b). Once the entire structure is released, the initial ~0.2% tensile strain redistributes such that the Ge pads relax slightly while the strain in the Ge wire increases, as confirmed by COMSOL finite element method modeling in Fig. 2(c).

 © 2014 Chinese Laser Press

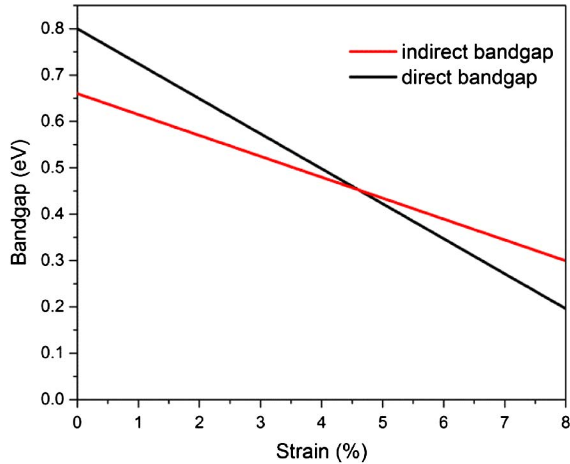

Fig. 1. Direct and indirect bandgaps of Ge as a function of ⟨100⟩ uniaxial tensile strain.

While using HF vapor etch successfully yields a suspended Ge wire under high tensile strain, this suspended geometry results in poor thermal conduction since there is no direct heat conduction path from the wire to the substrate. We have very recently shown that replacing the HF vapor etch of the underlying oxide with a liquid HF etch induces postrelease stiction that adheres the Ge wire and pads to the substrate [25], as shown in Fig. 3. This change does not reduce the strain induced in the wire, but placing the Ge wire in thermal contact with the substrate creates an efficient heat conduction path, which in turn drastically reduces any heating effects [25].

3. EXPERIMENTAL CHARACTERIZATION

The strain in the fabricated Ge wires was experimentally determined using Raman spectroscopy. Under tensile strain,

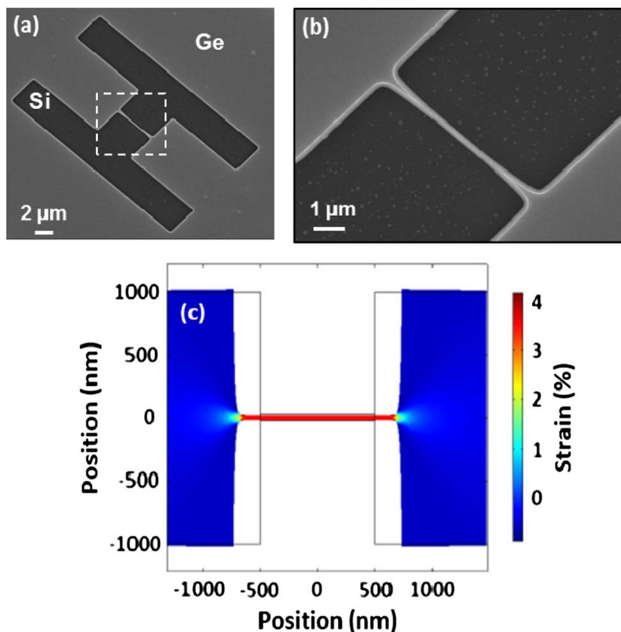

Fig. 2. (a) Scanning electron micrograph (SEM) of a suspended strained Ge wire attached to suspended Ge pads. (b) Zoomed-in SEM of the region indicated in (a). (c) COMSOL simulation of the strain distribution in a suspended Ge wire attached to suspended Ge pads.

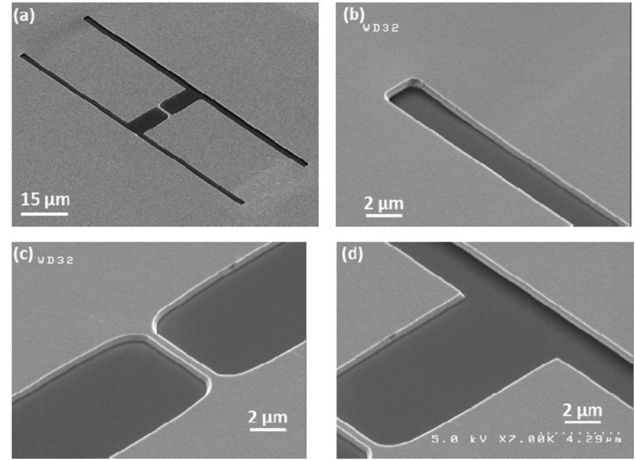

Fig. 3. (a) Tilted scanning electron micrograph (SEM) of a substrate-adhered strained Ge wire and pads. (b) Zoomed-in tilted SEM of the edge of a pad, showing deflection due to stiction. (c) Zoomed-in tilted SEM of the substrate-adhered Ge wire. (d) Zoomed-in titled SEM showing a substrate-adhered Ge wire and pads next to an overhang of suspended Ge.

the Raman peak of 301 cm^{-1} for relaxed Ge becomes redshifted to shorter wavenumbers: every 1% ⟨100⟩ uniaxial tensile strain redshifts the Raman peak by 1.52 cm^{-1} [19,26]. Using this Raman strain-shift coefficient of 152 cm^{-1} for ⟨100⟩ uniaxial strain corrects previous works [22,27], where the coefficient of 202 cm^{-1} for ⟨110⟩ uniaxial strain [28] was erroneously used instead. This caused all uniaxial strains to be underreported by ~25% in [22,27].

While the strain is a simple linear function of the Raman peak redshift, care must be taken to ensure that no significant heating occurs due to the excitation laser since temperature increases are also known to redshift the Raman peak. It is therefore critical to ensure that any observed Raman redshift corresponds to tensile strain rather than heating effects [26]. To this end, we have measured how the Raman peaks of both a suspended and a substrate-adhered Ge wire change with the Raman excitation laser power, as shown in Fig. 4. These wires had nominally identical dimensions and both exhibited approximately ~4% strain.

It is clear from Fig. 4 that Raman excitation laser powers below ~40 μW produce no significant heating effect in our suspended Ge wires. A laser excitation power of ~6 μW was therefore used in all subsequent Raman measurements, which is a factor of ~6.5 less than the maximum acceptable excitation power to avoid heating effects. Since our work on substrate-adhered wires is still in the early stages, we have yet to fabricate substrate-adhered wires with more than the ~4% strain shown in Fig. 4. However, our work on suspended wires is more mature, and we have observed substantially larger strains in these wires. Raman spectra of suspended wires with varying pad dimensions, shown in Fig. 5, reveal Raman peak locations as low as 292.37 cm^{-1}, compared to the Raman peak of 301.05 cm^{-1} for relaxed Ge. The observed redshifts of up to 8.68 cm^{-1} of the Raman peak correspond to uniaxial strains of up to 5.71% using the 152 cm^{-1} Raman strain-shift coefficient [19,26]. According to the deformation potentials for Ge [7], this largest observed strain of 5.71% corresponds to a direct bandgap of 0.369 eV and an indirect bandgap of 0.403 eV. This means that the bandgap of this 5.71%-strained Ge wire is direct.

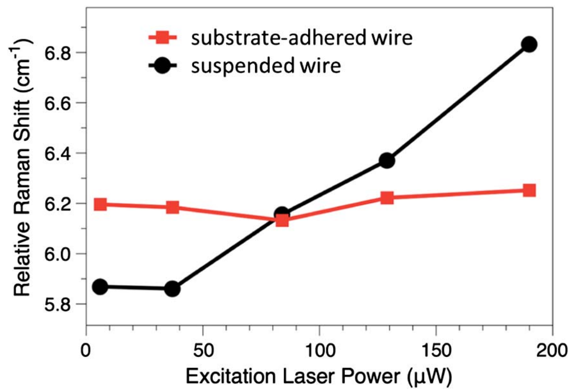

Fig. 4. Dependence of the Raman peak redshift on the excitation laser power for both suspended and substrate-adhered Ge wires with ~4% strain. Both curves are the difference between the wire's Raman peak location and the Raman peak location of relaxed bulk Ge.

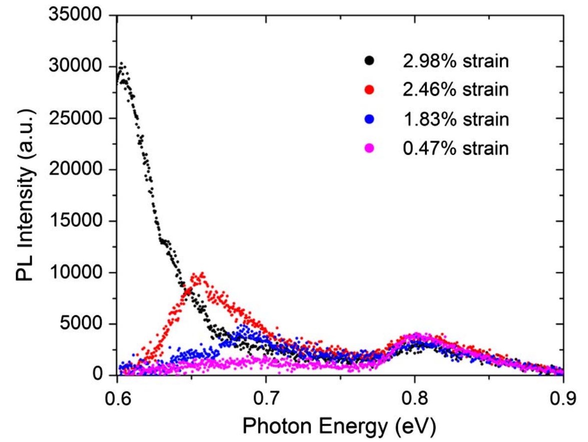

Fig. 6. Photoluminescence (PL) from suspended Ge wires with various strains.

In terms of optical properties, photoluminescence (PL) measurements on the suspended wires confirm that strain causes both a redshift of the emission wavelength due to the bandgap reduction and an enhancement of the PL intensity due to increased occupation of the direct conduction valley, as shown in Fig. 6. In fact, the PL intensity enhancement with strain is actually greater than the theoretical predictions of the following section due to pseudo-heterostructure effects between the pads and the wires as explained in [22]. This redshift and enhancement of the PL confirms that the strain is indeed affecting Ge's optical properties as expected.

Due to the limitations of our detection setup, PL from wires with strains beyond ~3% could not be measured because the emission was redshifted beyond the detector cutoff of ~2060 nm (0.6 eV photon energy) in our micro-PL setup. From Fig. 6 it is clear that even the 2.98% strained wire has been largely redshifted beyond this detection limit. Since only Ge wires with >4.6% strain have a direct bandgap, no optical measurements were possible on our direct bandgap Ge samples. We must therefore reserve such measurements for a future work.

4. THEORETICAL MODELING

While the achievement of a direct bandgap Group IV semiconductor directly integrated on Si is exciting in its own right, it is essential to understand the implications of such a material for Si photonics. Counterintuitively, even once a direct gap is achieved a large majority of electrons may still reside in the indirect conduction valleys. This is because the indirect valleys, being four-fold degenerate and having a much larger effective mass [12], collectively have a ~56× larger effective density of states (DOS) than the direct valley. At the direct gap crossover point of 4.6% strain, >98% of electrons will still reside in the indirect valleys (this percentage is determined by the DOS ratio of the valleys). The fraction of electrons in the direct conduction valley as a function of strain and temperature can be calculated, as shown in Fig. 7, by assuming parabolic bands and using Ge's deformation potentials [7]. Maxwell–Boltzmann statistics were used for this calculation since no doping or carrier injection was assumed, so the Fermi level can safely be assumed to be far below the conduction band edges.

From Fig. 7 it is clear that even though only 4.6% strain is sufficient to achieve a direct bandgap [7], a much larger strain of ~8.0% is required for >50% of electrons to reside in the direct valley at room temperature (300 K). Even at liquid nitrogen temperature (77 K), a strain of ~5.5% is required for >50% of electrons to reside in the direct valley, about ~0.9% strain more than the 4.6% needed for a direct bandgap. Only at liquid helium temperature (4 K) does the direct bandgap crossover even approximately coincide with the strain needed for the

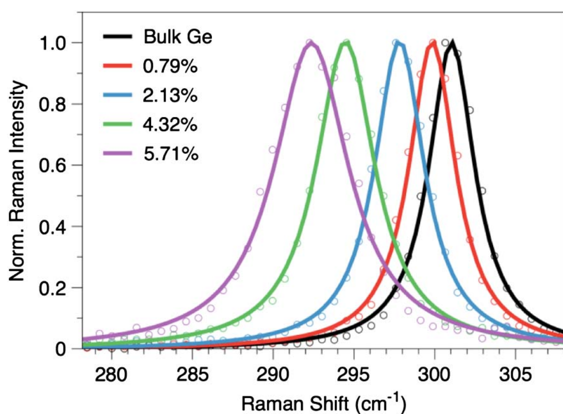

Fig. 5. Raman spectra for suspended Ge wires with various pad dimensions, showing uniaxial strains from 0.79% to 5.71%.

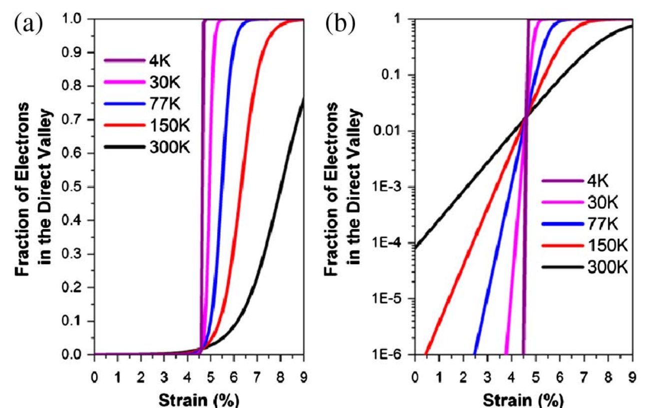

Fig. 7. Theoretically calculated fraction of electrons in the direct valley as a function of ⟨100⟩ uniaxial tensile strain, shown at several temperatures, plotted on a (a) linear scale and (b) logarithmic scale.

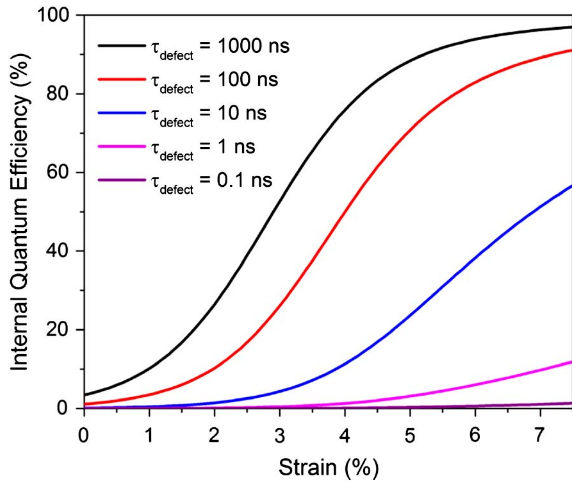

Fig. 8. Theoretical internal quantum efficiency of a Ge LED as a function of strain for various defect-limited minority carrier lifetimes at room temperature (300 K), assuming 10^{19} cm^{-3} n-type doping and 10^{17} cm^{-3} carrier injection.

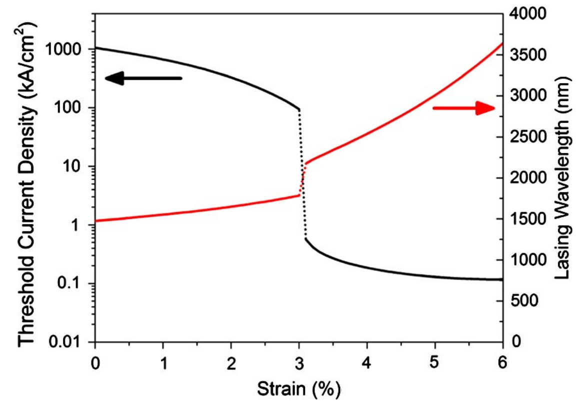

Fig. 9. Theoretically calculated threshold current density for a Ge laser as a function of strain.

direct conduction valley to be more populated than the indirect valleys. A corollary of this fact is that there is no sudden change to be expected in the optical properties of Ge once a direct gap is achieved, unless extremely low temperatures are employed.

However, even if only <50% of electrons reside in the direct valley, it is still possible for most recombination to be radiative due to the fast recombination coefficient for the direct valley [12] and picosecond-timescale intervalley scattering of electrons [29]. The latter property means that electrons will rapidly scatter from the indirect valley into the direct valley if a fast radiative recombination process occurs in the direct valley. Expanding upon the analysis of Fig. 7, it is possible to theoretically calculate the internal quantum efficiency of a Ge LED as a function of strain as shown in Fig. 8 for various defect-limited minority carrier lifetimes. This was done by calculating the fraction of recombination due to radiative transitions from the direct valley as opposed to other methods such as Auger and defect-based Shockley–Read–Hall (SRH) processes. The recombination coefficients for these processes were taken from [12]. Since most reported Ge LEDs employ substantial n-type doping, we have assumed 10^{19} cm^{-3} n-type doping in our analysis, which is in line with most reported devices [30–35], and an injected carrier density of 10^{17} cm^{-3}. Since doping is now present, Maxwell–Boltzmann statistics were no longer used and instead the Fermi–Dirac occupancy probability was numerically integrated over the DOS. It was also assumed that all recombination takes place in the Ge, i.e., a 100% injection efficiency in the LED.

From Fig. 8 it is clear that even when <2% of electrons reside in the direct conduction valley, radiative transitions from the direct valley will still be the dominant recombination process provided that the material is sufficiently defect-free. In this case, electrons will be scattering from the indirect conduction valley into the direct valley where they will eventually recombine. In addition, the strong dependence of the efficiency on the defect-limited minority carrier lifetime is a strong incentive to further minimize defects in the Ge by using a GOI approach such as ours, since GOI has generally been shown to have longer carrier lifetimes than traditional epitaxial Ge-on-Si, presumably due to defects [36].

The ultimate question, however, is how the presence of a direct bandgap will affect the performance of a Ge laser. This was modeled by extending the method we used in [25] to larger strains. Our model assumes parabolic bands along with the deformation potentials of [7]. For this calculation, we have assumed a double heterostructure laser with a 300 nm thick Ge active region, 10^{19} cm^{-3} n-type doping, and an ideal lossless cavity. Valence band mixing was included by assuming the top band has a heavy hole mass along the strain axis and a light hole mass along the other two axes, and vice versa for the second valence band. Here again there is no abrupt change in performance when the strain reaches the direct gap crossover of ~4.6%, assuming room temperature operation (300 K). There is, however, an abrupt decrease in the lasing threshold around 3.1% strain, shown as a discontinuity in Fig. 9. This feature is due to valence band splitting effects as explained in [17]: only past a certain strain is it possible for stimulated emission from the top valence band to by itself be sufficient to overcome free carrier losses. Lasing using only transitions to the top valence band reduces the lasing threshold since it is no longer necessary to fill the lower valence band with holes, though this also causes a larger redshift of the lasing wavelength [17,37], as seen in Fig. 8.

Our model shows that increasing the strain from zero to 5.7% reduces the threshold current density from ~1000 to ~0.1 kA/cm^2, an improvement of four orders of magnitude. As the strain approaches 6%, however, the predicted threshold current reaches a minimum beyond which strain provides no further benefit. This is due to both a saturation of direct valley occupancy, as shown in Fig. 7, and also to the deleterious effects of bandgap narrowing [38], particularly the fact that free carrier losses are greater at longer wavelengths. Since very large strains beyond ~6% will actually worsen a Ge laser's threshold, our fabricated samples with 5.7% strain represent close to the ultimate limit of desirable strain in Ge for this application.

5. DISCUSSION

By employing GOI substrates, we have achieved a record ⟨100⟩ uniaxial tensile strain of 5.7% in suspended Ge wires. Since 4.6% strain is believed to transform Ge into a direct bandgap semiconductor [7], these highly strained Ge wires represent a direct bandgap Group IV semiconductor integrated on Si. This strain was measured by Raman spectroscopy, and

great care was taken to ensure that the observed Raman shifts were not due to heating effects. Micro-PL measurements confirmed that the Ge wires with strains up to ~3% exhibited enhanced and redshifted emission as expected due to the lowering of the direct conduction valley relative to the indirect valley and the overall bandgap narrowing. Ge wires with >3% strain are also expected to show continued redshifts and enhancements of the PL; however, for >3% strain the PL emission is redshifted beyond our present detection capabilities. Optical measurements on our most highly strained Ge wires, including those with >4.6% strain, which we infer to have a direct bandgap, must therefore be reserved for a future work.

While the achievement of direct bandgap Ge is exciting, the implications are somewhat more subtle. Counterintuitively, we have shown theoretically that even once a direct bandgap is achieved at ~4.6% strain, most electrons will remain in the indirect conduction valleys due to their four-fold degeneracy and much larger effective masses. In fact, at room temperature a much larger strain of ~8.0% is needed for a majority of electrons to reside in the direct valley. For the observed 5.7% strain, for instance, only ~19% of electrons are expected to reside in the direct valley at 300 K despite the technically direct bandstructure. However, the extremely fast radiative recombination rate of the direct transition and the rapid scattering of electrons between conduction valleys mean that we nevertheless expect radiative direct gap recombination to be the dominant recombination process in a direct bandgap Ge, provided the material's defect-limited minority carrier lifetime is in the tens of nanoseconds or greater. This makes our direct bandgap Ge a promising candidate for Si-compatible infrared LEDs.

The critical application for strained Ge, however, is as a gain medium for a silicon-compatible laser. Here our highly strained direct bandgap Ge shows particular promise, with a >1000× threshold reduction expected compared to the present state-of-the-art electrically pumped Ge lasers [18]. While this level of strain would redshift any Ge laser's emission from 1550 to beyond 3000 nm, it is possible for some applications to operate at such wavelengths by simply redshifting the detection range of Ge by applying a similar strain to a Ge detector as proposed in [17,27]. Our modeling predicts that there is no sudden boost in performance to be expected upon reaching the direct gap crossover unless very low temperatures are employed; however, there is a very sharp reduction in the lasing threshold to be expected around ~3.1% strain due to valence band splitting effects as explained in [17]. Around 6% tensile strain, the lasing threshold actually reaches a minimum due to negative effects associated with the bandgap reduction such as increased free carrier losses at longer wavelengths as explained in [38]. This indicates that our 5.7% strained wires represent close to the ultimate limit of uniaxial tensile strain insofar as Ge laser applications are concerned.

ACKNOWLEDGMENTS

This work was supported by the U.S. Government through APIC Corporation (Dr. Raj Dutt), by the AFOSR MURI on Integrated Hybrid Nanophotonic Circuits (Grant No. FA9550-12-1-0024), and by a Stanford Graduate Fellowship. The authors thank Woo Shik Jung, Jae Hyung Lee, and Jan Petykiewicz of Stanford University for their assistance with sample fabrication. The authors also thank Martin J. Süess of ETH Zürich for his insights about determining the amount of tensile strain in Ge from Raman spectroscopy.

REFERENCES

1. K.-H. Koo, H. Cho, P. Kapur, and K. C. Saraswat, "Performance comparisons between carbon banotubes, optical, and Cu for future high-performance on-chip interconnect applications," IEEE Trans. Electron Devices **54**, 3206–3215 (2007).
2. D. A. B. Miller, "Rationale and challenges for optical interconnects to electronic chips," Proc. IEEE **88**, 728–749 (2000).
3. Y. Ishikawa and K. Wada, "Germanium for silicon photonics," Thin Solid Films **518**, S83–S87 (2010).
4. J. Liu, R. Camacho-Aguilera, J. T. Bessette, X. Sun, X. Wang, Y. Cai, L. C. Kimerling, and J. Michel, "Ge-on-Si optoelectronics," Thin Solid Films **520**, 3354–3360 (2012).
5. J. Liu, L. C. Kimerling, and J. Michel, "Monolithic Ge-on-Si lasers for large-scale electronic–photonic integration," Semicond. Sci. Technol. **27**, 094006 (2012).
6. P. Boucaud, M. El Kurdi, A. Ghrib, M. Prost, M. de Kersauson, S. Sauvage, F. Aniel, X. Checoury, G. Beaudoin, L. Largeau, I. Sagnes, G. Ndong, M. Chaigneau, and R. Ossikovski, "Recent advances in germanium emission," Photon. Res. **1**, 102–109 (2013).
7. C. G. Van de Walle, "Band lineups and deformation potentials in the model-solid theory," Phys. Rev. B **39**, 1871–1883 (1989).
8. L. Vivien, J. Osmond, J.-M. Fédéli, D. Marris-Morini, P. Crozat, J.-F. Damlencourt, E. Cassan, Y. Lecunff, and S. Laval, "42 GHz p.i.n Germanium photodetector integrated in a silicon-on-insulator waveguide," Opt. Express **17**, 6252–6257 (2009).
9. D. Nam, D. Sukhdeo, A. Roy, K. Balram, S.-L. Cheng, K. C.-Y. Huang, Z. Yuan, M. Brongersma, Y. Nishi, D. Miller, and K. Saraswat, "Strained germanium thin film membrane on silicon substrate for optoelectronics," Opt. Express **19**, 25866–25872 (2011).
10. J. Michel, J. Liu, and L. C. Kimerling, "High-performance Ge-on-Si photodetectors," Nat. Photonics **4**, 527–534 (2010).
11. J. E. Roth, O. Fidaner, R. K. Schaevitz, Y.-H. Kuo, T. I. Kamins, J. S. Harris, and D. A. B. Miller, "Optical modulator on silicon employing germanium quantum wells," Opt. Express **15**, 5851–5859 (2007).
12. J. Liu, X. Sun, D. Pan, X. Wang, L. C. Kimerling, T. L. Koch, and J. Michel, "Tensile-strained, n-type Ge as a gain medium for monolithic laser integration on Si," Opt. Express **15**, 11272–11277 (2007).
13. Y. Cai and R. Camacho-Aguilera, "High n-type doped germanium for electrically pumped Ge laser," in *Integrated Photonics Research, Silicon and Nanophotonics (IPRSN)* (Optical Society of America, 2012), pp. 5–7.
14. Y. Cai, R. Camacho-Aguilera, J. T. Bessette, L. C. Kimerling, and J. Michel, "High phosphorous doped germanium: dopant diffusion and modeling," J. Appl. Phys. **112**, 034509 (2012).
15. M. El Kurdi, G. Fishman, S. Sauvage, and P. Boucaud, "Band structure and optical gain of tensile-strained germanium based on a 30 band k·p formalism," J. Appl. Phys. **107**, 013710 (2010).
16. G. Capellini, G. Kozlowski, Y. Yamamoto, M. Lisker, T. Schroeder, A. Ghrib, M. de Kersauson, M. El Kurdi, P. Boucaud, and B. Tillack, "Tensile strained Ge layers obtained via a Si-CMOS compatible approach," in *International Silicon-Germanium Technology and Device Meeting (ISTDM)* (IEEE, 2012), pp. 1–2.
17. B. Dutt, D. S. Sukhdeo, D. Nam, B. M. Vulovic, Z. Yuan, and K. C. Saraswat, "Roadmap to an efficient germanium-on-silicon laser: strain vs. n-type doping," IEEE Photon. J. **4**, 2002–2009 (2012).
18. R. E. Camacho-Aguilera, Y. Cai, N. Patel, J. T. Bessette, M. Romagnoli, L. C. Kimerling, and J. Michel, "An electrically pumped germanium laser," Opt. Express **20**, 11316–11320 (2012).
19. M. J. Süess, R. Geiger, R. A. Minamisawa, G. Schiefler, J. Frigerio, D. Chrastina, G. Isella, R. Spolenak, J. Faist, and H. Sigg, "Analysis of enhanced light emission from highly strained germanium microbridges," Nat. Photonics **7**, 466–472 (2013).

20. J. R. Jain, D. Ly-Gagnon, and K. Balram, “Tensile-strained germanium-on-insulator substrate fabrication for silicon-compatible optoelectronics,” Opt. Mater. Express **1**, 1121–1126 (2011).
21. J. Liu, D. D. Cannon, K. Wada, Y. Ishikawa, S. Jongthammanurak, D. T. Danielson, J. Michel, and L. C. Kimerling, “Tensile strained Ge p-i-n photodetectors on Si platform for C and L band telecommunications,” Appl. Phys. Lett. **87**, 011110 (2005).
22. D. Nam, D. S. Sukhdeo, J.-H. Kang, J. Petykiewicz, J. H. Lee, W. S. Jung, J. Vučković, M. L. Brongersma, and K. C. Saraswat, “Strain-induced pseudoheterostructure nanowires confining carriers at room temperature with nanoscale-tunable band profiles,” Nano Lett. **13**, 3118–3123 (2013).
23. A. K. Okyay, A. M. Nayfeh, T. Yonehara, A. Marshall, P. C. McIntyre, and K. C. Saraswat, “Ge on Si by novel heteroepitaxy for high efficiency near infrared photodetection,” in *Conference on Lasers and Electro-Optics (CLEO)*, OSA Technical Digest (CD) (Optical Society of America, 2006), paper CTuU5.
24. T. Yi, L. Li, and C. Kim, “Microscale material testing of single crystalline silicon: process effects on surface morphology and tensile strength,” Sens. Actuators A **83**, 172–178 (2000).
25. D. Nam, D. Sukhdeo, and S. Gupta, “Study of carrier statistics in uniaxially strained Ge for a low-threshold Ge laser,” IEEE J. Sel. Top. Quantum Electron. **20**, 1500107 (2013).
26. M. J. Süess, ETH Zürich (Private Communication, 2013).
27. D. S. Sukhdeo, D. Nam, J.-H. Kang, J. Petykiewicz, J. H. Lee, W. S. Jung, J. Vu, M. L. Brongersma, and K. C. Saraswat, “Direct bandgap germanium nanowires inferred from 5.0% uniaxial tensile strain,” in *2013 IEEE 10th International Conference on Group IV Photonics (GFP)* (IEEE, 2013), Vol. **4**, pp. 73–74.
28. C.-Y. Peng, C.-F. Huang, Y.-C. Fu, Y.-H. Yang, C.-Y. Lai, S.-T. Chang, and C. W. Liu, “Comprehensive study of the Raman shifts of strained silicon and germanium,” J. Appl. Phys. **105**, 083537 (2009).
29. S. A. Claussen, E. Tasyurek, J. E. Roth, and D. A. B. Miller, “Measurement and modeling of ultrafast carrier dynamics and transport in germanium/silicon-germanium quantum wells,” Opt. Express **18**, 25596–25607 (2010).
30. S.-L. Cheng, G. Shambat, J. Lu, H.-Y. Yu, K. Saraswat, T. I. Kamins, J. Vuckovic, and Y. Nishi, “Cavity-enhanced direct band electroluminescence near 1550 nm from germanium microdisk resonator diode on silicon,” Appl. Phys. Lett. **98**, 211101 (2011).
31. M. Schmid, M. Oehme, M. Gollhofer, R. Körner, M. Kaschel, E. Kasper, and J. Schulze, “Effect of heavy doping and strain on the electroluminescence of Ge-on-Si light emitting diodes,” Thin Solid Films (in press).
32. M. de Kersauson, R. Jakomin, M. El Kurdi, G. Beaudoin, N. Zerounian, F. Aniel, S. Sauvage, I. Sagnes, and P. Boucaud, “Direct and indirect band gap room temperature electroluminescence of Ge diodes,” J. Appl. Phys. **108**, 023105 (2010).
33. P. Velha, K. Gallacher, D. Dumas, M. Myronov, D. Leadley, and D. Paul, “Direct band-gap electroluminescence from strained n-doped germanium diode,” in *Conference on Lasers and Electro-Optics*, OSA Technical Digest (online) (Optical Society of America, 2012), paper CW1L.7.
34. R. Camacho-Aguilera, J. Bessette, Y. Cai, L. C. Kimerling, and J. Michel, “Electroluminescence of highly doped Ge pnn diodes for Si integrated lasers,” in *8th IEEE International Conference on Group IV Photonics* (IEEE, 2011), pp. 190–192.
35. D. Nam, D. Sukhdeo, S.-L. Cheng, A. Roy, K. C.-Y. Huang, M. Brongersma, Y. Nishi, and K. Saraswat, “Electroluminescence from strained germanium membranes and implications for an efficient Si-compatible laser,” Appl. Phys. Lett. **100**, 131112 (2012).
36. R. Geiger, J. Frigerio, M. J. Suess, R. A. Minamisawa, D. Chrastina, G. Isella, R. Spolenak, J. Faist, and H. Sigg, “Excess carrier lifetimes in Ge layers on Si,” in *IEEE International Conference on Group IV Photonics* (IEEE, 2013), pp. 103–104.
37. D. S. Sukhdeo, H. Lin, D. Nam, Z. Yuan, B. M. Vulovic, S. Gupta, J. S. Harris, B. Dutt, and K. C. Saraswat, “Approaches for a viable germanium laser: tensile strain, GeSn alloys, and n-type doping,” in *2013 Optical Interconnects Conference* (IEEE, 2013), pp. 112–113.
38. D. Sukhdeo, D. Nam, Z. Yuan, B. Dutt, and K. Saraswat, “Toward an efficient germanium-on-silicon laser: ultimate limits of tensile strain and n-type doping,” in *Conference on Lasers and Electro-Optics (CLEO)*, OSA Technical Digest (online) (Optical Society of America, 2013), paper JTh2A.109.